



Published in final edited form as:

*Ophthalmol Glaucoma*. 2019 ; 2(1): 11–21. doi:10.1016/j.ogla.2018.11.010.

## Aqueous Angiographic Outflow Improvement after Trabecular Microbypass in Glaucoma Patients

Alex S. Huang<sup>1</sup>, Rafaella C. Penteado<sup>2</sup>, Vahan Papoyan<sup>3</sup>, Lilit Voskanyan<sup>3</sup>, Robert N. Weinreb<sup>2</sup>

<sup>1</sup>Doheny Eye Institute and Department of Ophthalmology, David Geffen School of Medicine at UCLA, Los Angeles, CA, USA

<sup>2</sup>Hamilton Glaucoma Center, Shiley Eye Institute, and Department of Ophthalmology University of California, San Diego, CA, USA

<sup>3</sup>Department of Ophthalmology, Yerevan State Medical University, Ophthalmological Center after S.V. Malayan

### Abstract

**Purpose:** To study changes in aqueous humor outflow (AHO) patterns after trabecular microbypass (TMB) in glaucoma patients using intraoperative sequential aqueous angiography.

**Design:** Prospective comparative case series

**Subjects:** Fifteen subjects (14 with glaucoma and 1 normal)

**Methods:** Sequential aqueous angiography (Spectralis HRA+OCT; Heidelberg Engineering) was performed on fourteen glaucoma patients undergoing routine TMB (iStent Inject; Glaukos Corporation) and cataract surgery and one normal patient undergoing cataract surgery alone. Indocyanine green (ICG) aqueous angiography established initial baseline nasal angiographic AHO patterns. Two TMB stents were placed in regions of baseline low or high angiographic AHO in each eye (n = 2 eyes with enough space to place two stents in both low angiographic regions; n = 8 eyes with two stents both placed in high angiographic regions; n = 4 eyes with enough space to place one stent in a low angiographic region and the other stent in a high angiographic region). Subsequent fluorescein aqueous angiography was utilized to query alterations to angiographic AHO patterns.

**Main Outcome Measure:** Angiographic signal and patterns before and after TMB.

**Results:** At baseline, all eyes showed segmental angiographic AHO patterns. Focused on the nasal hemisphere of each eye, for each stent TMB in initially low ICG angiographic signal regions showed transient or persistently improved fluorescein angiographic signal (11.2-fold;  $p = 0.014$ ).

---

**Corresponding Author:** Alex Huang, MD/PhD, Doheny Eye Institute, Department of Ophthalmology, David Geffen School of Medicine, University of California, Los Angeles, 1355 San Pablo Street, Los Angeles, CA 90033, Ahuang@Doheny.org, Phone: 323-442-6436; Fax: 323-442-6688.

**Publisher's Disclaimer:** This is a PDF file of an unedited manuscript that has been accepted for publication. As a service to our customers we are providing this early version of the manuscript. The manuscript will undergo copyediting, typesetting, and review of the resulting proof before it is published in its final citable form. Please note that during the production process errors may be discovered which could affect the content, and all legal disclaimers that apply to the journal pertain.

TMB in initially high ICG signal regions led to faster development of fluorescein angiographic patterns (3.1-fold;  $p = 0.02$ ).

**Conclusion:** TMB resulted in different patterns of aqueous angiographic AHO improvement whose further understanding may advance basic knowledge of AHO and possibly enhance intraocular pressure reduction after glaucoma surgery in the future.

## Abstract

After trabecular micro-bypass, sequential aqueous angiography showed that different types of aqueous humor outflow (AHO) improvement are possible in live glaucoma patients, including regions of initially low AHO being rescued.

## Introduction

New methods have emerged to image aqueous humor outflow (AHO) and AHO pathways. Histology<sup>1</sup> and 3D-micro CT<sup>2</sup> have been described in the laboratory. Optical coherence tomography (OCT)<sup>3-6</sup> has been performed in live human subjects. These methods demonstrate lumens capable of conducting aqueous humor in the anterior segment. However, structural evaluation alone can be misleading because not every lumen in the anterior segment necessarily carries aqueous humor<sup>7, 8</sup>. For example, pathways exist for lymph, arterial blood, and venous blood not associated with AHO. Also, the relationship between outflow structural variation to AHO behavior is unclear. Tracer-based studies, in which tracers are introduced into the eye to visualize fluid flow, provide an alternative and complementary approach for assessing AHO<sup>9-15</sup>.

Aqueous angiography is a new method that delivers tracers, such as fluorescein and indocyanine green (ICG) into the anterior chamber, that are imaged by an angiographic camera. Developed in the laboratory using post-mortem (pig<sup>16</sup>, cow<sup>17</sup>, cat [McLellan et al, 2018 ARVO C0195], and human<sup>16, 18</sup>) eyes and translated to live non-human primates<sup>19</sup> and humans<sup>20, 21</sup>, aqueous angiography has proven that AHO is segmental and non-uniform around the limbus. In humans, segmental AHO has a predilection toward the nasal hemisphere, supporting prior structural AHO investigation<sup>16, 18, 20-23</sup>. Additionally, aqueous angiography has shown that AHO is pulsatile<sup>19, 20</sup>, also consistent with previous anterior segment OCT (AS-OCT) research<sup>5</sup>. Lastly, aqueous angiography has shown that AHO is dynamic<sup>19, 20</sup>, by increasing and decreasing in different parts of the eye at various times. With aqueous angiography, it should be possible to gain an enhanced understanding of how the AHO pathways are influenced under different conditions including Minimally Invasive Glaucoma Surgeries (MIGS).

MIGS are a recent and commonly employed therapeutic option to facilitate AHO and lower intraocular pressure (IOP) in glaucoma patients. These procedures are safer, quicker, and have a smaller incision compared to conventional glaucoma surgeries. For most MIGS procedures, the trabecular meshwork (TM) undergoes ablation<sup>24, 25</sup> or trabecular micro-bypass (TMB)<sup>26-28</sup>.

Here, we use aqueous angiography to study the impact of trabecular MIGS on AHO. Using sequential aqueous angiography, it has been shown that introduction of intracameral ICG

followed by fluorescein in the same human eye demonstrates similar segmental angiographic patterns<sup>17, 18</sup>. Sequential tracer methods have also been applied to enucleated cow<sup>29</sup> and pig eyes<sup>30, 31</sup>. These approaches establish experimental paradigms to study outflow interventions such as IOP-lowering drugs or surgeries. For example, studied on post-mortem humans eyes in the lab, TMB has shown that low-angiographic signal regions can be improved<sup>18</sup>. First, ICG aqueous angiography was conducted to identify initially baseline low angiographic signal areas, and then TMB was performed there. Then, fluorescein aqueous angiography was conducted and showed that there was successful recruitment and development of new angiographic outflow patterns<sup>18</sup>.

Given that aqueous angiography has now been successfully translated to the operating room in normal human patients undergoing cataract surgery<sup>20, 21</sup>, the current study performed sequential aqueous angiography and compared angiographic patterns before and after TMB in glaucoma patients.

## Methods:

This study was carried out in accordance with the Declaration of Helsinki and approved by the Institutional Review Boards of University of California, San Diego and the Armenian Ministry of Health. Written informed consent was obtained.

## Test Subjects

Fifteen patients were consented for this study (68.3  $\pm$  1.9 years of age; mean  $\pm$  SEM; range 50-79 years; 4 men and 11 women; 6 right and 9 left eyes; 1 normal and 14 with glaucoma). Cataracts included nuclear sclerotic, posterior subcapsular, or both types. No patient had a known history of fluorescein, ICG, iodine, or shellfish allergies. All glaucoma patients had primary open angle glaucoma except one who had pseudoexfoliation glaucoma.

## Study Protocol

For glaucoma patients, only those already scheduled for combined cataract surgery with TMB were included. Aqueous angiography was performed in these patients over a 48-hour period in Armenia (February 2018). Previous literature had established greater AHO in the nasal hemisphere of the eye<sup>18-23</sup>, so recruiting a lesser number of glaucoma patients with low nasal angiographic AHO was expected. Thus, this study was not powered to identify intraocular pressure differences. The primary outcome was to investigate alterations in angiographic patterns.

In 14 glaucoma patients, aqueous angiography was performed (see below) with ICG to visualize the baseline angiographic AHO pattern in the nasal region of the eye. After ICG angiography, as the routine and approved method of surgery, two iStent Injects (Glaukos Corporation, USA) were placed ~ 2 clock hours apart under gonioscopic view. If large areas of low angiographic signal were seen in the nasal hemisphere, the iStent Injects were targeted to those locations. Otherwise, at least one was placed in a low nasal angiographic signal region with the other in a high nasal angiographic signal region. If there were no nasal low nasal angiographic regions, both stents were placed in high angiographic nasal signal regions. This was then followed by fluorescein aqueous angiography (see below) to query

the effect of the TMB before segueing into cataract surgery. One normal subject had ICG directly followed by fluorescein aqueous angiography and cataract surgery (without TMB).

### Aqueous Angiography and Surgical Steps

All subjects started with topical dilating drops (1% tropicamide and 2.5% phenylephrine, Akorn, IL, USA). Monitored anesthesia care was provided (including sedation and topical anesthetic) followed by surgical time-out, sterile-prep, drape, and placement of a lid speculum. Aqueous angiography imaging of the normal subject undergoing cataract surgery was performed as previously described<sup>20, 21</sup>. For glaucoma patients, two-port access was created to facilitate even-fluid exchanges (Fig. 1). Two Lewicky AC-maintainers (20g [K20-3276], Katena, NJ, USA), primed with sterile balanced salt solution (BSS; Alcon) normally used for cataract surgery, were inserted through 1mm side-port wounds supero-temporal and infero-temporal in each eye. After placement, both AC maintainers were capped with BSS-primed 1cc syringes to maintain no flow into or out of the eye.

Pharmaceutical-grade 25% fluorescein (AK-Fluor 25% [NDC17478-25-20], Akorn) was diluted to 2% with sterile room-temperature BSS. Pharmaceutical-grade indocyanine green (ICG, ICGREEN 25 mg [NDC 17478-701-25], Akorn) was thoroughly dissolved to 0.4% by adding 0.7 ml of the manufacturer provided sterile solvent followed by 5.6 ml of sterile BSS. These concentrations were chosen based on prior experience in enucleated cow<sup>17</sup> and human<sup>16, 18</sup> eyes; intact and living non-human primate<sup>19</sup> and human<sup>20, 21</sup> eyes; and because they have been described for clinical use at these concentrations in live humans as intraocular capsular stains to assist the capsulorhexis during cataract surgery<sup>32</sup>.

Aqueous angiographic images were acquired by the Spectralis FLEX Module (Heidelberg Engineering GmbH, Heidelberg, Germany) in the operating room. The Spectralis FLEX Module is a modified surgical arm that allows for stable three-dimensional manipulations and positioning of the Spectralis HRA+OCT (Heidelberg Engineering GmbH, Heidelberg, Germany) camera head relative to the supine patient's eye via multiple pivot joints. Alignment of the camera along the z-axis was controlled by an integrated micro-manipulator. Next to the head rest, an IV pole was sterile draped (General Purpose Probe Cover [PC1289], Ecolab, MN, USA) and placed on the side of the eye to be imaged. This pole held three syringe reservoirs, each with a stop-cock, situated ~10 inches above the eye to provide a gravity-delivered constant pressure of ~18.7 mm Hg for BSS, fluorescein, and ICG.

From this position, the Spectralis FLEX camera head was placed above the eye, and confocal scanning laser ophthalmoscopic (cSLO) infrared (IR) images were acquired to center the eye in the picture frame using a 55-degree lens (~25 diopter focus). Fluorescence images were obtained using the fluorescein capture mode (excitation wavelength: 486 nm and transmission filter set at > 500 nm) or ICG capture mode (excitation wavelength: 786 nm and transmission filter set at > 800 nm) to establish a pre-injection background that appeared black. After tracer introduction, IR and angiographic images were acquired immediately posterior to the limbus, near to where Schlemm's canal is located, with the subject looking in different directions.

The specific angiographic steps were as follows (Fig. 1). To start ICG aqueous angiography and introduce the tracer, the tubing from the ICG reservoir was connected to one AC maintainer. To initiate fluid exchange, the second AC maintainer was uncapped and held below the level of the eye to create unidirectional flow of ICG into the eye and aqueous out of the eye via the second AC maintainer. The second AC maintainer was then capped to build pressure in the eye and ICG angiographic imaging commenced as described above. After ICG aqueous angiography and to clear the tracer, the first AC maintainer was connected to the BSS reservoir, and the second AC maintainer uncapped and held below the level of the eye to initiate unidirectional flow of BSS into the eye and ICG out of the eye via the second AC maintainer. The second AC maintainer was capped to build pressure in the eye. The patient was then instructed to look nasal while the microscope tilted temporal. The tip of the iStent Inject hand-piece was inserted into the eye through a 1.5 mm temporal incision. The angle and trabecular meshwork were visualized using a gonioscope, and TMB performed in the prescribed locations. No viscoelastic was used as the BSS reservoir provided a pressure head for chamber stability. After TMB, the subject was instructed to look forward and the microscope returned vertical. The first AC maintainer was then connected to the fluorescein reservoir. The second AC maintainer was uncapped and held below the level of the eye to initiate unidirectional flow of fluorescein into the eye and BSS out of the eye via the second AC maintainer. The second AC maintainer was capped to build pressure in the eye and fluorescein angiographic imaging commenced. After fluorescein aqueous angiography, all AC maintainers were removed. BSS was introduced into the eye via a cannula to flush out the fluorescein, and viscoelastic was injected before transitioning to routine cataract surgery. At the end of the case, all wounds were hydrated or a suture placed for water tight closure.

### Aqueous Angiography Image Analyses

Aqueous angiographic images were analyzed similar to previous publications<sup>16-18</sup>. To compare the development of initial angiographic signal for each tracer in each eye, images were exported from the Spectralis and opened in Photoshop CS5 (v.12×32) for image processing and pixel intensity measurements. Additionally, to standardize the comparison between ICG and fluorescein despite different angiographic start-times with each tracer in each eye, the angiographic patterns in the first minute after signal initiation (~0, 10, 30, and 60 seconds) were compared. Because of subject motion, images were analyzed from as close to these time points as possible. In all images, “background signal intensity” was measured using a 75 × 75 square-pixel box placed over a region without angiographic signal and away from targeted TMB locations. Then, there were two image analysis approaches based on whether the TMB were placed in initially low- or high-ICG angiographic regions. For cases where TMB was placed in low ICG-angiographic regions, the same 75 × 75 square pixel box was placed post-limbal near-adjacent TMB locations on ICG and fluorescein images at the final time-point (~60 second image). The signal intensity of each was then divided by the “background signal intensity” from the same image to obtain a normalized signal intensity ratio. This controlled for varying sensitivity settings on the Spectralis that were adjusted during image acquisition to minimize signal-oversaturation. In other words, by dividing the signal intensity in the region of interest by background signal intensity from the same image, setting changes on the device could be controlled for. Therefore, a normalized signal

intensity ratio of ~1 (no units as this is a ratio) would imply that the signal in the test region of interest was no different from background. Statistical comparison between the ICG and fluorescein normalized signal ratios were then performed with a two-sample, equal-sized, and paired, Student's T-test (Microsoft Excel 2010). For eyes that had high and uniform initial nasal ICG-angiographic signal, the above analyses would not work. Both ICG and fluorescein signals were uniformly high at the ~60 second time point. Therefore, for each tracer, the same normalized signal intensity ratios near TMB regions were determined just as above except that this was done at every time point (~0, 10, 30, and 60 seconds after initiation of angiographic signal). These values were plotted over time, and the slope (or rate) of the signal intensity ratio increase was obtained (change in normalized signal intensity ratio over time; units = change in ratio/seconds). Slopes were compared between ICG and fluorescein aqueous angiography using a two-sample, equal-sized, and paired, Student's T-test. All data are expressed as mean +/- standard error.

## Results:

As an example, sequential aqueous angiography in a normal individual during cataract surgery without TMB showed similar results between the two tracers (Fig. 2). ICG and fluorescein showed similar regions with (green arrows) and without (red arrows) angiographic signal arising at comparable pace. These results replicated findings using the same experimental paradigm in laboratory post-mortem human eyes to show that TMB could improve regions of low aqueous angiographic outflow patterns<sup>18</sup>.

In 14 glaucoma subjects, sequential aqueous angiography was performed during cataract surgery and TMB with no complications. In these patients, average pre-operative IOP was 21.2 +/- 0.7 mm Hg, 24.5 +/- 0.8 mm Hg after a 1-week drug holiday, and 11.4 +/- 0.3 mm Hg at post-operative month 3.

In these patients, the average time for ICG aqueous angiography to show a signal (anywhere on the eye) was 33.7 +/- 4.6 seconds. After TMB, fluorescein aqueous angiography first showed signal (anywhere on the eye) at 26.9 +/- 3.8 seconds. The angiographic signal start-time was not statistically different comparing ICG and fluorescein ( $p = 0.28$ ) as the initial signal sometimes appeared away from the nasal hemisphere or where TMB was conducted. Therefore, in order to study the angiographic impact of TMB (that was only performed on the nasal hemisphere of the eye), we investigated the post-limbal angiographic AHO signal on the nasal portion of the eye and just adjacent to where TMB was performed. Additionally, to standardize the comparison between ICG and fluorescein despite different angiographic start-times with each tracer in each eye, the angiographic patterns in the first minute after signal initiation (~0, 10, 30, and 60) were compared.

### Trabecular Micro-Bypass (TMB) in Initially Low ICG-Angiographic Regions

In two cases, there were large enough regions of low nasal ICG angiographic signal (Fig. 3; red arrows) to accommodate placement of two TMB stents ~2 clock-hours apart (Fig. 3; blue arrows). After TMB, fluorescein aqueous angiography demonstrated development of new angiographic signal (Fig. 3; green arrows = "new recruitment"). In the first subject, this was particularly clear as infero-nasal there was pigment on the cornea creating a fluorescence



shadow that served as a reference point (Fig. 3B/F; black arrows). TMB was performed next to this reference point, and baseline ICG angiography clearly showed no post-limbal signal (Fig. 3D; red upper arrow). After TMB, fluorescein angiography showed the new angiographic pattern (Fig. 3H; green upper arrow).

In two other cases, regions of low ICG angiographic signal were more restricted and only one stent could be targeted to low ICG angiographic regions (Fig. 4). These examples supported the above in that TMB still led to new fluorescein aqueous angiographic signal recruitment (Fig. 4; green arrows). However, when placed next to a region with prior ICG angiographic signal (Fig. 4; orange arrows), instead of showing a new fluorescein angiographic pattern, the same patterns would emerge faster and brighter (Fig. 4; yellow arrows = “earlier recruitment”). These results suggested that each TMB site can be independent of each other as different types of improvement (new vs. earlier recruitment) could be seen, even in the same eye.

Another two cases demonstrated that TMB in initially low ICG angiographic signal regions did not always lead to new and robust fluorescein aqueous angiographic signal. In the first case, it appeared that TMB (Fig. 5D; lower blue arrow) did not lead to “new recruitment.” However, careful observation at very early time points showed initially new, albeit transient, recruitment of fluorescein angiographic signal (Fig. 5I-L; green arrows). Interestingly, in the same eye, TMB (Fig. 5D; higher blue arrow) near a baseline ICG angiographic pattern (Fig. 5; orange arrow) led to “earlier recruitment” of the same angiographic pattern using fluorescein (Fig. 5; yellow arrows). This again supported that each TMB location can behave independently of each other.

In the second case, TMB in a low ICG angiographic region (Fig. 6D; lower blue arrow) did not lead to improved fluorescein angiographic signal (Fig. 6D; red arrows), even at earlier time frames (data not shown). However, in this eye, the second TMB stent (Fig. 6; higher blue arrow) was again near a baseline ICG angiographic pattern (Fig. 6; orange arrow) and showed evidence of “earlier recruitment” using fluorescein (Fig. 6; yellow arrows).

In total, 8 TMB stents were placed in 6 eyes in clearly low ICG angiographic regions with results ranging between no alteration to new or earlier angiographic AHO. The average post-operative month 3 IOP was 11.7 mm  $\pm$  0.7 mm Hg. To quantify the impact of TMB, normalized ICG and fluorescein angiographic signal intensity ratios were determined at ~ 60 sec after initiation of angiographic signal (see methods and Fig. 3C). In these glaucoma patients, fluorescein normalized angiographic signal intensity ratios obtained after TMB were 11.2-fold greater than ICG normalized angiographic signal intensity ratios obtained before TMB (fluorescein: 15.7  $\pm$  4.8; ICG: 1.4  $\pm$  0.5;  $p = 0.014$ ).

### **Trabecular Micro-Bypass (TMB) in Initially High ICG-Angiographic Regions**

In the 6 eyes above, the remaining 4 TMB regions represented examples of “earlier recruitment.” This phenomenon was also seen in cases where baseline nasal ICG angiographic signal was uniform ( $n = 8$  subjects with 16 TMB stents) such that there was no low-signal region available to perform TMB. In these eyes, the average post-operative month 3 IOP was 11.3  $\pm$  0.4 mm Hg and not statistically different ( $p = 0.57$ ) from above where at

least one stent was successfully placed in a low angiographic signal region. This may be as TMB in initially high-ICG angiographic signal regions still showed “earlier recruitment.” TMB performed near baseline ICG angiographic patterns (Fig. 7; orange arrow) showed faster and brighter signal using fluorescein (Fig. 7; yellow arrows). To assess the rate of increase, ICG and fluorescein normalized angiographic signal intensity ratios were obtained at each time-point and plotted over time. Combining the data, the average elevation in signal intensity was relatively linear (ICG  $r^2 = 0.968$  and fluorescein  $r^2 = 0.975$ ). Comparing the exact same locations in the eyes, fluorescein aqueous angiography after TMB showed a faster rate (18.2 +/- 4 ratio/min) of signal increase compared to ICG aqueous angiography obtained before TMB (5.8 +/- 2 ratio/min;  $p = 0.02$ ).

## Discussion

For the first time, aqueous angiography was performed in glaucoma patients simultaneously undergoing TMB with cataract surgery. Baseline aqueous angiography in these glaucoma patients continued to show segmental angiographic AHO patterns. Post-limbal regions around the eye could have more or less angiographic AHO. The segmental AHO patterns were consistent with previous literature showing segmental uptake of fluorescent microbeads in the trabecular meshwork<sup>10, 12, 15</sup> These results also supported observations of segmental aqueous angiographic AHO demonstrated in live normal humans<sup>20, 21</sup>, live non-human primates<sup>19</sup>, and post-mortem pig<sup>16</sup>, cow<sup>17</sup>, cat (McLellan et al, 2018 ARVO C0195), and human eyes<sup>16, 18</sup>.

Current results also showed robust nasal aqueous angiographic AHO. Only 2/14 eyes had enough nasal area of low ICG angiographic signal to accommodate two TMB stents placed ~2 clock-hours apart. An additional 4/14 eyes had enough nasal area of low ICG angiographic signal where one TMB stent could be confidently placed. The remaining 8/14 eyes had robust nasal and near uniform baseline ICG angiographic signal with no areas of low angiographic signal for TMB placement. This preponderance of strong nasal angiographic AHO was consistent with previous literature showing that structural AHO pathways were more present on the nasal hemisphere of the eye<sup>22, 23</sup>. These results also supported prior aqueous angiographic results from live non-human primates<sup>19</sup> and normal humans<sup>20, 21</sup> demonstrating more angiographic AHO on the nasal hemisphere of the eye.

In this study, the primary purpose was to conduct two-dye sequential aqueous angiography before and after TMB. Now, tracer studies during glaucoma surgery have been previously performed where trypan blue was introduced after trabecular ablation<sup>33</sup>. In this case, imaging was conducted after surgical ablation using just one tracer. Thus, there could be no prior knowledge as to whether the trabecular ablation was placed in a region of initial low or high segmental AHO. The question<sup>33</sup> was focused on whether trabecular ablation could lead to any observable outflow using a tracer. Here, because of the sequential aqueous angiographic approach, the question was different. The primary outcome was whether there were alterations to initial angiographic AHO patterns as a consequence of TMB.

Replicating prior experimental design in post-mortem human eyes<sup>18</sup> (TMB performed between two angiography using different tracers), similar results were seen in this study with



live glaucoma patients. After TMB, angiographic AHO improvement was demonstrated, and in particular there were different types of improvement. In regions of low baseline ICG angiographic signal, “new recruitment” of fluorescein angiographic signal was documented just as in post-mortem human eye experiments. This could be persistent or transient. In other cases, where ICG aqueous angiography showed the presence of baseline angiographic signal patterns, TMB in those areas could lead to earlier or stronger fluorescein angiographic signal. The biological underpinnings of different types of responses are currently unknown, although trabeculotomized *ex vivo* eyes have continued to show resistance changes in response to vasoactive agents<sup>34</sup>. Therefore, distal AHO pathway regulation maybe partially responsible for the spectrum of responses that were recorded.

While TMB could improve angiographic AHO patterns and signal, how these results relate to IOP reduction in glaucoma patients undergoing TM-based MIGS is not yet clear. In this report, all patients showed some type of angiographic improvement, and all patients demonstrated IOP reduction. It is also important to emphasize that the primary purpose and outcome in this study was to study changes in angiographic patterns. To study IOP, consistent with clinical trials, a larger sample size would be needed to have enough power to detect significant differences. Also, to study IOP, a two-tracer experimental paradigm would not even be necessary. In fact, it would make the experiments more difficult because the second tracer and extra time for tracer delivery would lead to more corneal staining that would diminish the gonioscopic view critical for TMB. To study IOP, a more streamlined approach would consist of conducting angiography with one tracer, identify regions of high or low angiographic signal, and then placing the TMB in either one of these two regions. Lastly, in the current experiments, the results specifically looked at angiographic pattern changes before leaving the operating room in the immediate intra-operative period after TMB. Ideally, we could follow these subjects over time and repeat angiography in the future with correlation to IOP; however, there is often no clinical indication to re-enter the eye. Alternatively, anterior segment optical coherence tomography in angiographically altered regions is another way to follow what happens over time. These results may help understand but can't entirely explain why some patients have longer-lasting or stronger IOP lowering after surgery. Post-surgical healing, scarring, deposition of biological material<sup>35</sup>, and additional factors likely also contribute to the long-term final IOP outcome after trabecular MIGS.

An additional limitation in this study was that aqueous humor dynamic parameters were not measured real-time during the procedure. It is possible that pressure perturbations in the current approach altered the normal physiology of AHO pathways. However, as a study done as a part of routine clinical care, the subjects required excellent visual outcomes. Therefore, time was limited and the exact pressures during exchange, time interval, and volumes were not measured. Taking this type of research in a more controlled direction, animal studies would be one place to start where more sophisticated experimental designs requiring more time and manipulation could be performed.

Despite these limitations, it is clear that in both live and post-mortem human eyes<sup>18</sup>, regions of segmentally low angiographic signal can be rescued by TMB. This result is also consistent with the observation of dynamic angiographic outflow seen in live non-human

primates<sup>19</sup> and live humans<sup>20</sup>. Dynamic outflow showed that regions with or without initial angiographic signal can bi-directionally decrease or increase through yet unidentified mechanisms<sup>19, 20</sup>. Therefore, areas of the eye without angiographic outflow are not necessarily permanently so and can be improved either by TMB or through dynamic change. The regulation of whether a region of the eye supports AHO at any given time could occur at (or in any combination of) the trabecular meshwork, collector channels, intrascleral venous plexus, aqueous veins, and/or episcleral veins. Current IOP lowering drugs might already be targeting multiple components of this pathway.

In conclusion, this study demonstrates that TMB can improve AHO, as assessed by aqueous angiography. Different patterns or types of improvement are seen. Understanding these behaviors during surgery may lead to improved IOP reduction through targeted placement of TMB in optimal locations. Exploring these native behaviors in the eye may unveil previously unrecognized points of outflow regulation. Studying the molecular governance of how regions of outflow can dynamically change may lead to novel future pharmacological targets for IOP lowering.

## Acknowledgements

Funding for this work came from National Institutes of Health, Bethesda, MD (Grant Numbers K08EY024674 [ASH] and R01EY029058 [RNW]); Research to Prevent Blindness Career Development Award 2016 [ASH]; an unrestricted grant from Research to Prevent Blindness [UCLA and UCSD] (New York, NY), Glaukos Corporation, and Heidelberg Engineering who provided the Spectralis FLEX module. The funders had no role in study design, data collection and analysis, decision to publish, or preparation of the manuscript.

## References

1. DVORAK-THEOBALD G, KIRK HQ Aqueous pathways in some cases of glaucoma. *Am J Ophthalmol* 1956;41(1):11–21. [PubMed: 13275540]
2. Hann CR, Bentley MD, Vercnocke A, et al. Imaging the aqueous humor outflow pathway in human eyes by three-dimensional micro-computed tomography (3D micro-CT). *Exp Eye Res* 2011;92(2): 104–11. [PubMed: 21187085]
3. Kagemann L, Wollstein G, Ishikawa H, et al. Visualization of the conventional outflow pathway in the living human eye. *Ophthalmology* 2012;119(8):1563–8. [PubMed: 22683063]
4. Huang AS, Belghith A, Dastiridou A, et al. Automated circumferential construction of first-order aqueous humor outflow pathways using spectral-domain optical coherence tomography. *J Biomed Opt* 2017;22(6):66010. [PubMed: 28617922]
5. Li P, Shen TT, Johnstone M, Wang RK. Pulsatile motion of the trabecular meshwork in healthy human subjects quantified by phase-sensitive optical coherence tomography. *Biomed Opt Express* 2013;4(10):2051–65. [PubMed: 24156063]
6. Skaat A, Rosman MS, Chien JL, et al. Effect of Pilocarpine Hydrochloride on the Schlemm Canal in Healthy Eyes and Eyes With Open-Angle Glaucoma. *JAMA Ophthalmol* 2016;134(9):976–81. [PubMed: 27347646]
7. Marvasti AH, Berry J, Sibug ME, et al. Anterior Segment Scleral Fluorescein Angiography in the Evaluation of Ciliary Body Neoplasm: Two Case Reports. *Case Rep Ophthalmol* 2016;7(1):30–8. [PubMed: 26889157]
8. SUGAR HS, RIAZI A, SCHAFFNER R The bulbar conjunctival lymphatics and their clinical significance. *Trans Am Acad Ophthalmol Otolaryngol* 1957;61(2):212–23. [PubMed: 13422475]
9. Swaminathan SS, Oh DJ, Kang MH, et al. Secreted protein acidic and rich in cysteine (SPARC)-null mice exhibit more uniform outflow. *Invest Ophthalmol Vis Sci* 2013;54(3):2035–47. [PubMed: 23422826]

10. Cha ED, Xu J, Gong L, Gong H. Variations in active outflow along the trabecular outflow pathway. *Exp Eye Res* 2016.
11. Grieshaber MC, Pienaar A, Olivier J, Stegmann R. Clinical evaluation of the aqueous outflow system in primary open-angle glaucoma for canaloplasty. *Invest Ophthalmol Vis Sci* 2010;51(3):1498–504. [PubMed: 19933180]
12. Battista SA, Lu Z, Hofmann S, et al. Reduction of the available area for aqueous humor outflow and increase in meshwork herniations into collector channels following acute IOP elevation in bovine eyes. *Invest Ophthalmol Vis Sci* 2008;49(12):5346–52. [PubMed: 18515571]
13. Huang AS, Francis BA, Weinreb RN. Structural and functional imaging of aqueous humour outflow: a review. *Clin Exp Ophthalmol* 2018;46(2):158–68. [PubMed: 28898516]
14. Huang AS, Mohindroo C, Weinreb RN. Aqueous Humor Outflow Structure and Function Imaging At the Bench and Bedside: A Review. *J Clin Exp Ophthalmol* 2016;7(4).
15. Keller KE, Bradley JM, Vranka JA, Acott TS. Segmental versican expression in the trabecular meshwork and involvement in outflow facility. *Invest Ophthalmol Vis Sci* 2011;52(8):5049–57. [PubMed: 21596823]
16. Saraswathy S, Tan JC, Yu F, et al. Aqueous Angiography: Real-Time and Physiologic Aqueous Humor Outflow Imaging. *PLoS One* 2016;11(1):e0147176. [PubMed: 26807586]
17. Huang AS, Saraswathy S, Dastiridou A, et al. Aqueous Angiography with Fluorescein and Indocyanine Green in Bovine Eyes. *Transl Vis Sci Technol* 2016;5(6):5.
18. Huang AS, Saraswathy S, Dastiridou A, et al. Aqueous Angiography-Mediated Guidance of Trabecular Bypass Improves Angiographic Outflow in Human Enucleated Eyes. *Invest Ophthalmol Vis Sci* 2016;57(11):4558–65. [PubMed: 27588614]
19. Huang AS, Li M, Yang D, et al. Aqueous Angiography in Living Nonhuman Primates Shows Segmental, Pulsatile, and Dynamic Angiographic Aqueous Humor Outflow. *Ophthalmology* 2017.
20. Huang AS, Camp A, Xu BY, et al. Aqueous Angiography: Aqueous Humor Outflow Imaging in Live Human Subjects. *Ophthalmology* 2017.
21. Huang AS, Penteado RC, Saha SK, et al. Fluorescein Aqueous Angiography in Live Normal Human Eyes. *J Glaucoma* 2018.
22. Kagemann L, Wollstein G, Ishikawa H, et al. Identification and assessment of Schlemm's canal by spectral-domain optical coherence tomography. *Invest Ophthalmol Vis Sci* 2010;51(8):4054–9. [PubMed: 20237244]
23. Johnstone M, Jamil A, Martin E. Aqueous Veins and Open Angle Glaucoma In: Schacknow PN, Samples JR, eds. *The Glaucoma Book: A Practical, Evidence-Based Approach to Patient Care*. New York: Springer, 2010.
24. Akil H, Chopra V, Huang A, et al. Clinical results of ab interno trabeculotomy using the Trabectome in patients with pigmentary glaucoma compared to primary open angle glaucoma. *Clin Exp Ophthalmol* 2016;44(7):563–9. [PubMed: 26946187]
25. Akil H, Chopra V, Huang AS, et al. Short-Term Clinical Results of Ab Interno Trabeculotomy Using the Trabectome with or without Cataract Surgery for Open-Angle Glaucoma Patients of High Intraocular Pressure. *J Ophthalmol* 2017;2017:8248710. [PubMed: 28484649]
26. Malvankar-Mehta MS, Chen YN, Iordanous Y, et al. iStent as a Solo Procedure for Glaucoma Patients: A Systematic Review and Meta-Analysis. *PLoS One* 2015;10(5):e0128146. [PubMed: 26018579]
27. Lindstrom R, Lewis R, Hornbeak DM, et al. Outcomes Following Implantation of Two Second-Generation Trabecular Micro-Bypass Stents in Patients with Open-Angle Glaucoma on One Medication: 18-Month Follow-Up. *Adv Ther* 2016;33(11):2082–90. [PubMed: 27739003]
28. Berdahl J, Voskanyan L, Myers JS, et al. Implantation of two second-generation trabecular micro-bypass stents and topical travoprost in open-angle glaucoma not controlled on two preoperative medications: 18-month follow-up. *Clin Exp Ophthalmol* 2017;45(8):797–802. [PubMed: 28384377]
29. Zhu JY, Ye W, Gong HY. Development of a novel two color tracer perfusion technique for the hydrodynamic study of aqueous outflow in bovine eyes. *Chin Med J (Engl)* 2010;123(5):599–605. [PubMed: 20367989]

30. Parikh HA, Loewen RT, Roy P, et al. Differential Canalograms Detect Outflow Changes from Trabecular Micro-Bypass Stents and Ab Interno Trabeculectomy. *Sci Rep* 2016;6:34705. [PubMed: 27811973]
31. Loewen RT, Brown EN, Scott G, et al. Quantification of Focal Outflow Enhancement Using Differential Canalograms. *Invest Ophthalmol Vis Sci* 2016;57(6):2831–8. [PubMed: 27227352]
32. Jacobs DS, Cox TA, Wagoner MD, et al. Capsule staining as an adjunct to cataract surgery: a report from the American Academy of Ophthalmology. *Ophthalmology* 2006;113(4):707–13. [PubMed: 16581432]
33. Laroche D, Nortey A, Ng C. A Novel Use of Trypan Blue During Canalicular Glaucoma Surgery to Identify Aqueous Outflow to Episcleral and Intrasceral Veins. *J Glaucoma* 2018.
34. McDonnell F, Dismuke WM, Overby DR, Stamer WD. Pharmacological regulation of outflow resistance distal to Schlemm's canal. *Am J Physiol Cell Physiol* 2018;315(1):C44–C51. [PubMed: 29631366]
35. Shah M, Campos-Möller X, Werner L, et al. Midterm failure of combined phacoemulsification with trabecular microbypass stenting: Clinicopathological analysis. *J Cataract Refract Surg* 2018;44(5):654–7. [PubMed: 29891158]

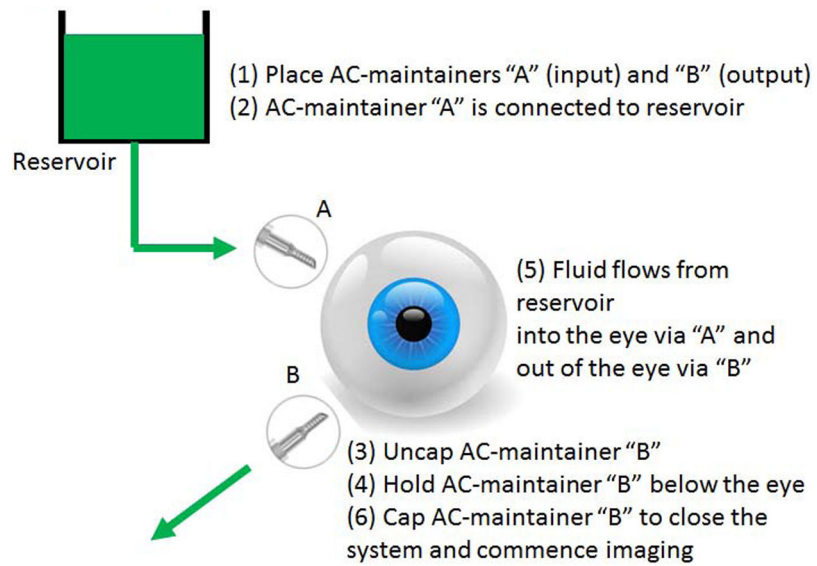


**Figure 1. Aqueous Angiography Perfusion System**

Sequential steps (1-6) spell out the process of delivering tracer (fluorescein or indocyanine green) or balanced salt solution into the eye.

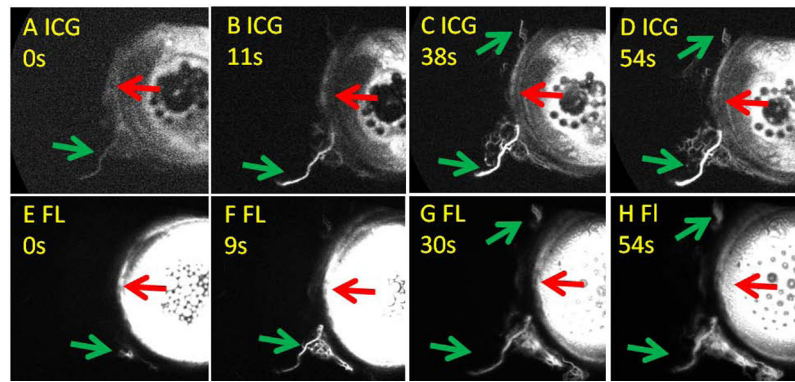


**Figure 2. Sequential Aqueous Angiography in a Normal Subject.**

A-D) Aqueous angiography with indocyanine green (ICG) was performed first. E-H) Aqueous angiography with fluorescein (FL) was conducted immediately after the ICG angiography. Green arrows point out regions with post-limbal angiographic signal. Red arrows point out regions without post-limbal angiographic signal. s = seconds after signal initiation.



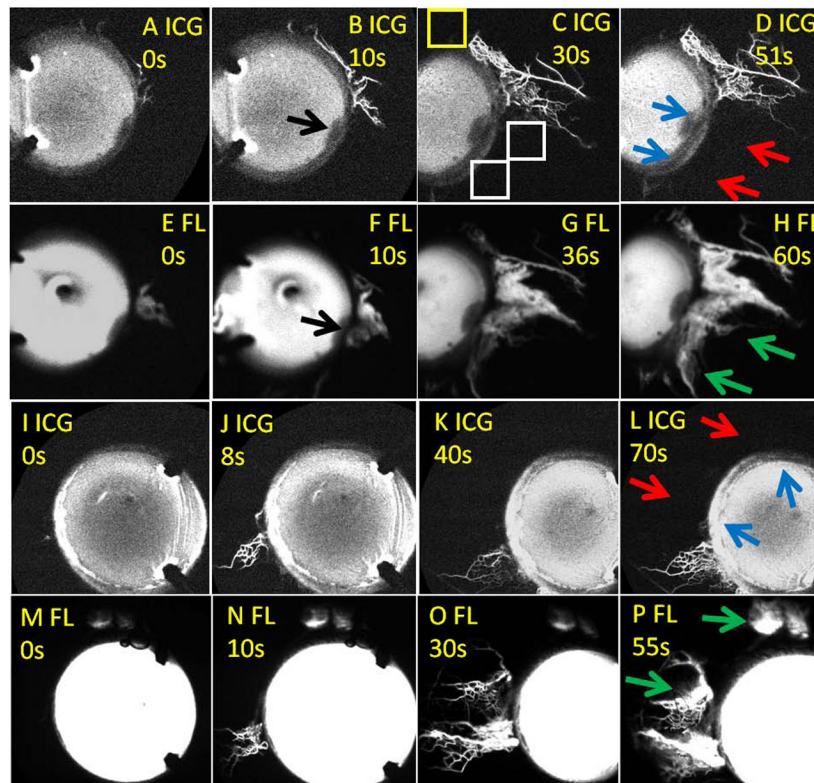


**Figure 3. Sequential Aqueous Angiography in Glaucoma Patients with TMB in Initially Low Outflow Regions Showing New Angiographic Patterns.**

(A-H) The first patient. (I-P) The second patient. (A-D and I-L) First, indocyanine green (ICG) aqueous angiography was performed. D/L) Second, TMB was conducted (blue arrows). (E-H and M-P) Third, fluorescein (FL) aqueous angiography was performed immediately after TMB. (B/F) In the first patient, black arrows point out conjunctival pigment on the cornea that blocked fluorescence transmission. This location serves as a reference point across all images for that eye. D/L) Red arrows point out nasal regions of the eyes without initial ICG angiographic signal. H/P) Green arrows point out regions of new fluorescein angiographic signal after TMB. (C) This image serves as an example of how to calculate an angiographic signal intensity ratio. A  $75 \times 75$ -pixel region of interest was placed post-limbal near the region of TMB (white boxes). Then for each region of interest, the signal intensity was normalized by dividing it by the signal in a region of known background away from proposed areas of TMB (yellow box). This allowed for assessment of signal intensity in any image, internally normalized to the settings on the Spectralis. A ratio of 1 would imply that the signal intensity in that region of interest was no different than the background. Because these values were ratios, they have no units. s = seconds after signal initiation.

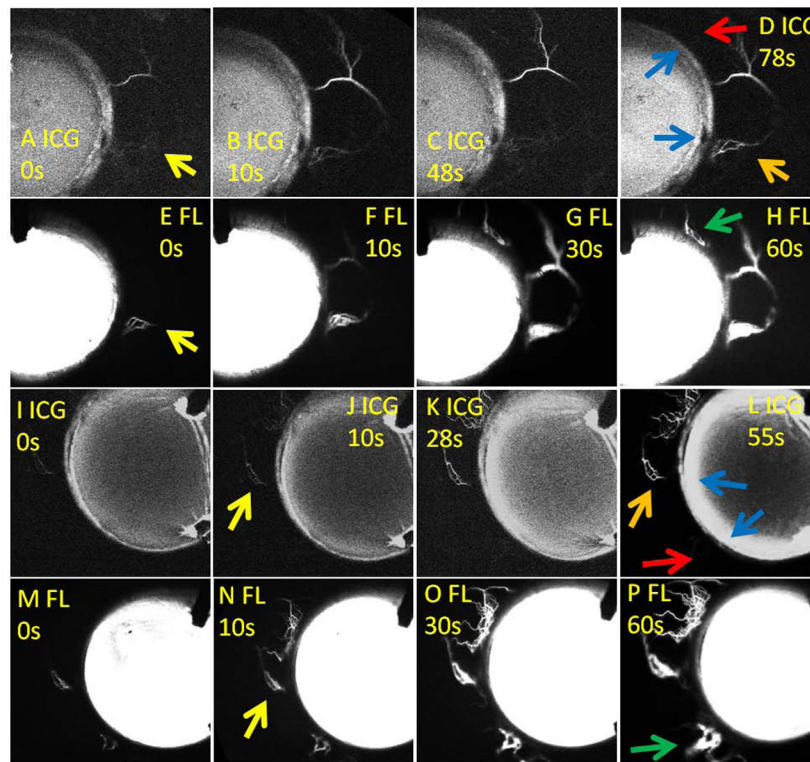


**Figure 4. Sequential Aqueous Angiography in Glaucoma Patients with TMB Showing New or Earlier Signal Development**

(A-H) The first patient. (I-P) The second patient. (A-D and I-L) First, indocyanine green (ICG) aqueous angiography was performed. D/L) Second, TMB was conducted (blue arrows). (E-H and M-P) Third, fluorescein (FL) aqueous angiography was performed immediately after TMB. In the first patient, the upper TMB location (D; upper blue arrow) had a larger area for insertion into a low ICG angiographic region. The lower TMB (D; lower blue arrow) was placed ~ 2 clock hours inferior and close to a pre-existing ICG angiographic structure (D; orange arrow). In the second patient, the lower TMB location (L; lower blue arrow) had a larger area for insertion into a low ICG angiographic region. The upper TMB location (L; upper blue arrow) was placed ~ 2 clock hours superior and close to a pre-existing ICG angiographic structure (L; orange arrow). Red arrows (D/L) point out regions with initially low ICG angiographic signal that showed the development of new fluorescein angiographic patterns (H/P, green arrows) after TMB. Yellow arrows demonstrate nasal regions of the eye that had ICG angiographic signal (D/L; orange arrows) which appeared earlier on fluorescein angiography after TMB (E/N [fluorescein] vs. A/J [ICG]). s = seconds after signal initiation.

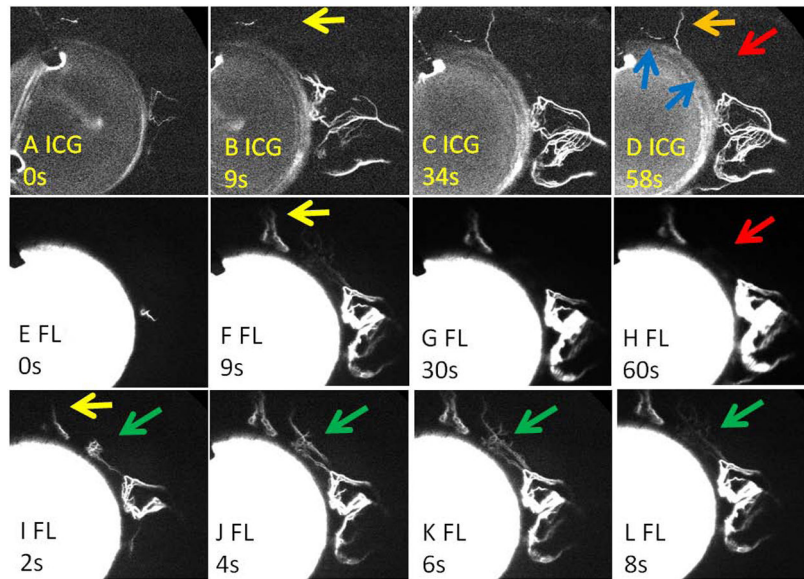


**Figure 5. Sequential Aqueous Angiography in a Glaucoma Patient with TMB Showing Transient and Earlier Signal Development.**

A-D) First, indocyanine green (ICG) aqueous angiography was performed. D) Second, TMB was conducted (blue arrows). The lower TMB location (D; lower blue arrow) had a large enough area for insertion into a low ICG angiographic region. The upper TMB (D; upper blue arrow) was placed ~ 2 clock hours superior and close to a pre-existing ICG angiographic structure (D; orange arrow). (E-H) Fluorescein (FL) aqueous angiography was performed immediately after TMB. Red arrows show a nasal region of the eye (D) without initial ICG angiographic signal that (H) did not appear to improve after TMB. I-L) However, fluorescein angiography between 2-8 seconds after TMB did show a transiently appearing new angiographic pattern in the initially low ICG angiographic region (green arrows). Yellow arrows demonstrate nasal regions of the eye that had initial ICG angiographic signal (D; orange arrow) which appeared earlier on fluorescein angiography after TMB (F/I [fluorescein] vs. B [ICG]). s = seconds after signal initiation.

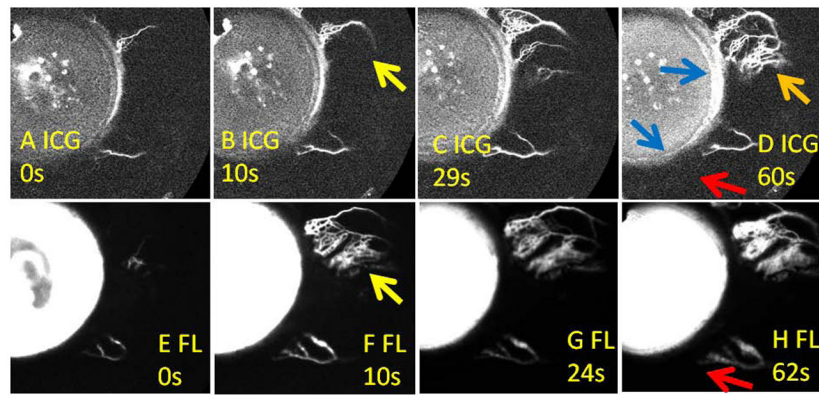


**Figure 6. Sequential Aqueous Angiography in a Glaucoma Patient with TMB Showing No Alteration and Earlier Signal Development.**

A-D) First, indocyanine green (ICG) aqueous angiography was performed. D) Second, TMB was conducted (blue arrows). The lower TMB location (D; lower blue arrow) had a large enough area for insertion into a low ICG angiographic region. The upper TMB (D; upper blue arrow) was placed ~ 2 clock hours superior and close to a pre-existing ICG angiographic structure (D; orange arrow). (E-H) Fluorescein (FL) aqueous angiography was performed immediately after TMB. Red arrows show a nasal region of the eye (D) without initial ICG angiographic signal that (H) did not improve after TMB. Yellow arrows demonstrate a nasal region of the eye that had ICG angiographic signal (D; orange arrow) which appeared earlier on fluorescein angiography after TMB (F [fluorescein] vs. B [ICG]). s = seconds after signal initiation.

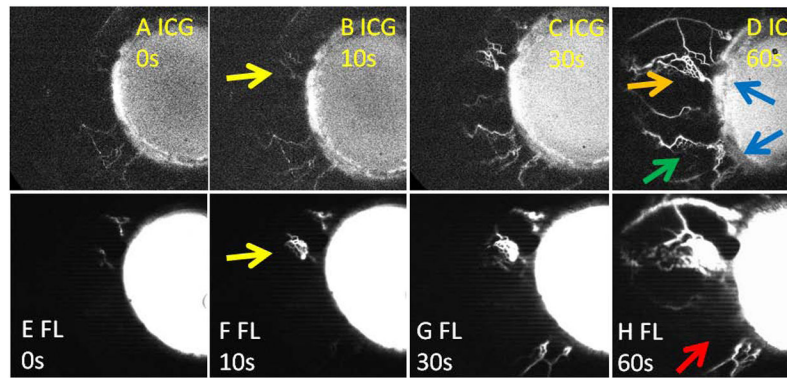


**Figure 7. Sequential Aqueous Angiography in a Representative Glaucoma Patient with TMB in Initially High Outflow Regions.**

A-D) First, indocyanine green (ICG) aqueous angiography was performed. Note uniform nasal ICG angiographic signal (D) such that there were no low angiographic signal regions to place TMB. D) Second, TMB was conducted (blue arrows). (E-H) Third, fluorescein (FL) aqueous angiography was performed immediately after TMB. The lower TMB (D; lower blue arrow) demonstrate initial ICG angiographic signal (D; green arrow) that did not improve after TMB (H; red arrow). Yellow arrows demonstrate nasal regions of the eye that had ICG angiographic signal (D; orange arrow) which appeared earlier on fluorescein angiography after TMB (F [fluorescein] vs. B [ICG]). s = seconds after signal initiation.